Measurement of the Branching Ratio: $R=[(\pi^+ \rightarrow \pi^0+e^++\nu_e)/(\pi^+ \rightarrow \mu^++\nu_\mu)]$*

WILLIAM K. BERTRAM† AND DONALD I. MEYER
University of Michigan, Ann Arbor, Michigan

AND

RICHARD A. CARRIGAN, JR., AND IRVING NADELHAFT
Carnegie Institute of Technology, Pittsburgh, Pennsylvania

(Received 25 March 1965)

The branching ratio for pion beta decay $[R=(\pi^+ \rightarrow \pi^0+e^++\nu_e)/(\pi^+ \rightarrow \mu^++\nu_\mu)]$ has been measured with a system of spark chambers and scintillation counters. The high spatial resolution of the spark chambers was used to measure the position of the stopping pion as well as the angle between the nearly back-to-back gamma rays arising from the decay of the neutral pion. A total of 95×10^9 positive pions was stopped in a central polystyrene-plate spark chamber. After measurement, computation, and background subtraction, the experiment yielded 35 ± 3 pion beta-decay events. These were used with the over-all efficiency of the apparatus (about 3.3%) to compute a branching ratio $R=(1.10\pm0.26)\times10^{-8}$. The result is in agreement with the predictions of the conserved-vector-current theory.

I. INTRODUCTION

THE conserved-vector-current hypothesis[1] (CVC) was introduced to explain the fact that the vector-coupling constant in beta decay $g_V{}^\beta$ is not renormalized in the presence of strong interactions of the baryons involved in the decay process. This conclusion is based upon experimental evidence[2] attesting to the near equality of $g_V{}^\beta$ and the vector-coupling constant $g_V{}^\mu$ involved in muon decay. The difference between the coupling constants is usually expressed by the quantity $\gamma\equiv(g_V{}^\mu-g_V{}^\beta)/g_V{}^\mu$ which has the value[3] $\gamma=(2.2\pm0.2)\%$. In addition to the equality of $g_V{}^\beta$ and $g_V{}^\mu$, CVC predicts the existence of a magnetic interaction[4] in beta decay, the so-called weak magnetism. Several experiments designed to detect the effects of this contribution have been performed.[5] All of these bear out the predictions of CVC to an accuracy of about 10% and provide strong support for the theory.

Another consequence of CVC is an accurate prediction of the rate of the pion beta-decay reaction:

$$\pi^+ \rightarrow \pi^0+e^++\nu. \tag{1}$$

The branching ratio of pion beta decay to ordinary pion decay given by CVC is[6]

$$R\equiv\frac{\pi^+ \rightarrow \pi^0+e^++\nu}{\pi^+ \rightarrow \mu^++\nu}=(1.04\pm0.02)\times10^{-8}. \tag{2}$$

The $\pi^+\beta$ decay would be expected to occur even if CVC theory were not valid, through the existence of a virtual particle loop. However, attempts[7] to calculate the branching ratio on this basis are beset with the usual divergence difficulties although an attack[8] using dispersion theory gives results comparable to CVC.

The vector-coupling constant enters implicitly into the calculation of R and for the value given in (2), the coupling constant from muon decay has been used. Recently, Cabibbo[9] has pointed out that one should possibly use the beta-decay-vector constant. Since the coupling constant enters quadratically and since the discrepancy between the two constants is about 2.2%, this suggestion has the effect of lowering R approximately 5%, resulting in

$$R_{\text{Cabibbo}}=(0.99\pm0.02)\times10^{-8}. \tag{3}$$

When the experiment to be described here was begun, pion beta decay had been observed by several laboratories,[10] using techniques different from ours. Very few events were obtained in these first attempts because of the relative rareness of the process, and the results were in agreement with CVC although they had relatively large errors. More recently, the CERN group,[11] using an expanded apparatus (to increase the detection efficiency), has been able to accumulate about 165 events resulting in a value for R with an accuracy of 10%. Their number $R=(1.17\pm0.12)\times10^{-8}$ is slightly higher than the CVC values given in (2) and

* Supported in part by the U. S. Atomic Energy Commission.

† A thesis based upon this work has been submitted by William K. Bertram to the Department of Physics, University of Michigan, in partial fulfillment of the requirements for the degree of Doctor of Philosophy.

[1] R. P. Feynman and M. Gell-Mann, Phys. Rev. **109**, 193 (1958) and S. S. Gershtein and Ia. B. Zel'dovich, Zh. Eksperim. i Teor. Fiz. **29**, 698 (1955) [English transl.: Soviet Phys.—JETP **2**, 576 (1956)].

[2] R. K. Bardin, C. A. Barnes, W. A. Fowler, and P. A. Seeger, Phys. Rev. **127**, 583 (1962).

[3] J. M. Freeman, J. H. Montague, G. Murray, R. E. White, and W. E. Burcham, Phys. Letters **8**, 115 (1964).

[4] See, for example, C. S. Wu, Rev. Mod. Phys. **36**, 618 (1964).

[5] An excellent summary of these experiments appears in Ref. 4.

[6] M. V. Terent'ev, Zh. Eksperim. i Teor. Fiz. **44**, 1320 (1963) [English transl.: Soviet Phys.—JETP **17**, 890 (1963)], and Ngee-Pong Chang, Phys. Rev. **131**, 1272 (1963).

[7] E. Feenberg and H. Primakoff, Phil. Mag. **3**, 328 (1958).

[8] I. Duck, Nucl. Phys. **45**, 243 (1963).

[9] N. Cabibbo, Phys. Rev. Letters **10**, 531 (1963).

[10] P. DePommier, J. Heintze, C. Rubbia, and V. Soergel, Phys. Letters **5**, 61 (1963); A. F. Dimaritsev, V. I. Petrubkhin, Yu. D. Prokoshkin, and V. I. Rykalin, International Conference on Weak Interactions, BNL-837, 1963, p. 344 (unpublished); R. Bacastow, University of California Radiation Laboratory Report No. UCRL-10864, 1963 (unpublished).

[11] P. DePommier, J. Duclos, J. Heintze, K. Kleinknecht, H. Rieseberg, and V. Soergel, *International Conference on High Energy Physics, Dubna* (Moscow, 1964).

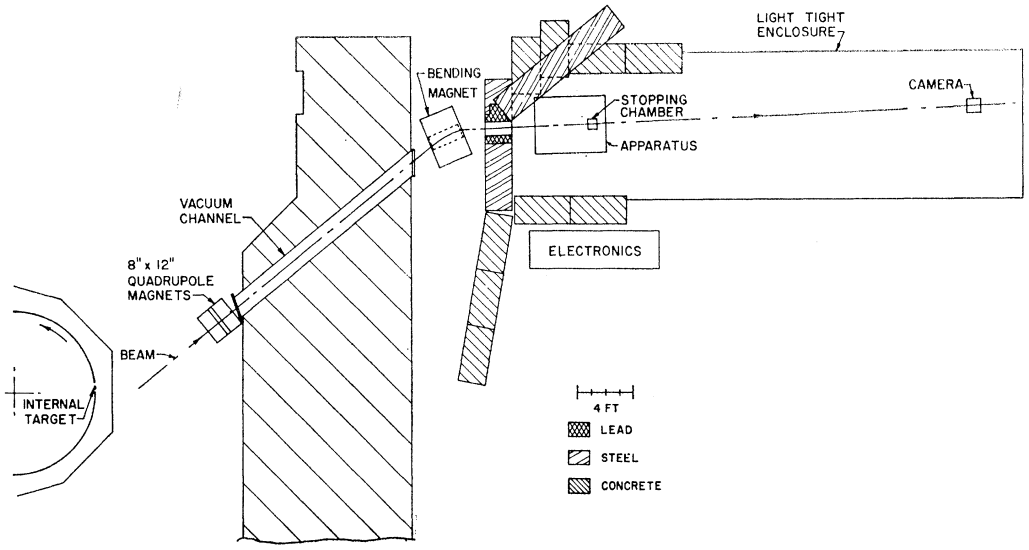

FIG. 1. Plan view of apparatus.

(3). Also recently, a group at Columbia,[12] using spark chambers in an arrangement similar to ours, has reported 36 events and a value for R, with 20% accuracy in agreement with CVC.

We describe here an experiment which also uses an apparatus consisting of spark chambers. In Sec. II we describe the apparatus and the beam. Section III discusses the data collected and the methods used to analyze them, while Sec. IV gives the results and comparisons with other experiments.

II. APPARATUS AND BEAM

A. The Spark Chambers and Electronics System

The pion beta-decay reaction (1) was selected by detecting the gamma rays, resulting from the π^0 decay, in delayed coincidence with a stopping pion. The low momentum of the neutral pion in this reaction ($P_{\max}=4.51$ MeV/c) results in gamma rays which are moving in almost opposite directions from one another. The minimum value of the opening angle $\theta_{\gamma\gamma}$ between them is 176.2° [$\cos(176.2°)=-0.998$]. The measurement of $\theta_{\gamma\gamma}$ was accomplished by stopping the positive pion in a small spark chamber and detecting the gamma rays, by converting them into electron-positron pairs, in two large spark chamber-scintillation counter systems. Figures 1 and 2 show the floor plan and details of the apparatus. A suitable reference frame can be defined by choosing a right-handed coordinate system with z along the beam direction, y up, and x horizontal. Beam particles were brought to rest (signature $123\bar{4}$) in a spark chamber whose area transverse to the beam was 6 in.×8 in. The chamber was constructed of polystyrene (CH) plates, 0.25 in. thick, which were separated from each other by Lucite frames, forming 16 gaps, each of which was 0.25 in. thick. Both sides of the polystyrene plates had faces made of 0.001-in. aluminum sheets which were glued to the plate, and served as the electrical surfaces in the spark chamber.

A $123\bar{4}$ coincidence generated a gate whose width was 50 nsec and which was delayed by approximately 10 nsec from the time of the stop (prompt time). The gate delay of 10 nsec guarded against "prompt" events. During the time the gate was open, coincidences between the top and bottom γ counters were accepted. Gamma rays emerging from the stopping point were converted and detected by a sandwich consisting of lead plates 0.050 in. thick, scintillation counters, and spark chambers. Going out from the central spark chamber the sequence consisted of: anticoincidence counter (lead, spark chamber, scintillant), with the group in parentheses repeated 8 times. Each γ detector contained 8 lead plates or about two radiation lengths, and each spark chamber had two 0.25-in. gaps and dimensions of 20 in.×34 in. The gaps were formed by 0.030-in. aluminum sheets glued to Lucite frames.

The scintillants were connected in two interleaving groups and a coincidence demanded between them. A gamma ray converting in the top chamber therefore was indicated by $\gamma_{T1}\gamma_{T2}A_T\equiv\gamma_T$ and a similar signature was used for the bottom detector. The simultaneous conversion of gamma rays in the top and the bottom was denoted by $\gamma_T\gamma_B\bar{1}\bar{\gamma}_T\bar{\gamma}_B\equiv\gamma\gamma$. The $\bar{1}\bar{\gamma}_T\bar{\gamma}_B$ pulse vetoed an event if a beam particle was coincident with the two gammas.

The different views of all the spark chambers in the apparatus were photographed on a single frame through a 4-ft-diam Lucite lens with a focal length of about 25 ft.

An event ($\pi\gamma\gamma$) was defined by a coincidence between

[12] D. Bartlett, S. Devons, S. L. Meyer, and J. L. Rosen, Phys. Rev. **136**, B1452 (1964).

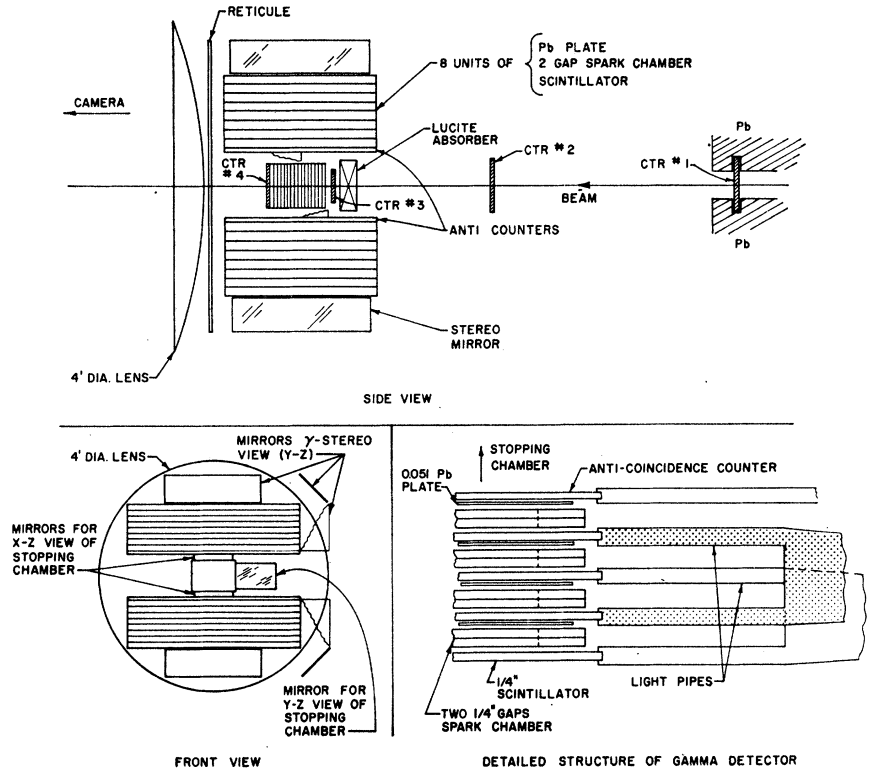

FIG. 2. Details of the apparatus.

a delayed gate, derived from a $123\bar{4}$ coincidence, and a $\gamma\gamma$ pulse. A $\pi\gamma\gamma$ trigger initiated a sequence of processes: (a) The spark chambers were fired and photographed; (b) an oscilloscope displaying various pulses (described below) was photographed; (c) all circuits were blocked for a period of two seconds to allow the recording mechanism and the spark-chamber high-voltage supply to recover.

The oscilloscope carried a display of the various γ detector counters, the anticoincidence counters, and the beam counter 3. The scope pictures could be matched against the spark-chamber photographs and provided a convenient cross check on the electronic selection. In particular, the operation of the anticoincidence counters could be checked and double stops, which had not been vetoed by $\bar{1}\bar{\gamma}\bar{\gamma}$, could be detected. Time information was obtained by measuring the distance between 3 and the γ pulses.

The spark chambers were filled with a Ne-He gas mixture (equal parts of each) which was allowed to flow continuously at a very low rate. The gas flow was monitored by a system of reduction valves, flow meters and bubblers arranged so that each 2-gap γ chamber was individually fed. This ensured adequate flow and resulted in reliable sparking efficiency. The spark chambers were energized by a system of four gaps. Top γ, bottom γ, and the stopping chamber each used one spark gap and these three spark gaps were all fired from a master trigger gap which in turn was triggered by the $\pi\gamma\gamma$ pulse through a driver circuit.

B. The Beam

Particles were produced by protons striking an internal-carbon target in the Carnegie Tech synchrocyclotron and were curved by the cyclotron-fringing field through a quadrupole pair (8-in. aperture), down a beam port, containing a vacuum pipe, and bent by a dipole into the stopping particle telescope. Positive or negative particles were selected by choosing the polarity of the magnets. The beam was spread over time by an electronic stretcher.[13] The resulting beam had uniform intensity over the cyclotron repetition time of 5 msec except for a very small portion (about 100 μsec) during which there was an enhanced intensity. This 100-μsec region was gated out during the performance of the experiment. The beam retained some of its original fine structure derived from the cyclotron radio frequency accelerating voltage (the period is 50 nsec). The beam intensity resulted in a steady rate of $123\bar{4}$ coincidences of about 60 000 per second of either positive or negative particles.

It is necessary to know the fraction of stops which were pions since stopping particles could also be muons or electrons. This knowledge was needed for negative particles as well as positive particles because, as will be shown later, data taken with negative pions were used to determine the efficiency of the γ detectors. The composition of the beam was carefully investigated in

[13] M. H. Foss, R. W. Findley, and A. Suzuki, Nucl. Instr. Methods **92**, 282 (1964).

a series of little experiments in which electrons, muons, and pions were measured as a function of range. Some techniques were employed in addition to the straightforward separation obtained from a range curve. Electrons and positrons were detected with a Čerenkov counter which was not sensitive to muons and pions; negative pions were measured with the π-star method,[14] and negative and positive muons were measured using a detector sensitive to the electrons from muon decay. From all these data it was possible to determine what function of the $123\bar{4}$ counts corresponded to pions which came to rest in that particular section of the stopping chamber which was used as the final fiducial region.

III. DATA AND ANALYSIS

A. General Considerations

The branching ratio R, Eq. (2), is related to the measured events by the equation

$$N_{\pi\beta}=N_{\pi}{}^{+}R\epsilon_{g}\epsilon^{+}. \tag{3}$$

$N_{\pi\beta}$ is the number of acceptable events which remain after the pictures have been scanned, measured, computed, and the various acceptance criteria applied, and after background has been subtracted, i.e., these are considered to be instances where a pion has decayed as in (1). $N_{\pi}{}^{+}$ is the number of positive pions which have stopped in the chosen fiducial volume of the middle spark chamber. This number is derived from the scalar count of $123\bar{4}$ coincidences after the application of corrections for beam contamination, multiple stops, and fiducial volume. ϵ_g is the probability that a pion decay took place within the π gate. ϵ^{+} is the efficiency for detecting the gamma rays resulting from the π^0 decay. This efficiency is a composite of many factors including geometry, conversion efficiency, electronics efficiency, and will be discussed in detail below.

Of all of these factors, the efficiency ϵ^{+} is crucial and in order to determine its value another reaction was studied, the charge exchange of negative pions at rest on hydrogen:

$$\pi^{-}+p\rightarrow\pi^{0}+n. \tag{4}$$

The hydrogen for this reaction was contained in the Polystyrene (chemical composition CH) which made up plates of the middle spark chamber. Negative pions were brought to rest in the spark chamber and the gamma rays from π^0 decay detected in coincidence with the $123\bar{4}$ signature indicating a stopping particle. An equation similar to (3) can be written

$$N_{ce}=N_{\pi}{}^{-}R_{ce}\epsilon^{-}. \tag{5}$$

N_{ce} is the number of acceptable charge-exchange events after analysis. $N_{\pi}{}^{-}$ is the number of negative pions which stopped in the fiducial volume. R_{ce} is the branching ratio for reaction (4). This number has been measured[12,15] and is found to be $R_{ce}=(3.3\pm0.3)\times10^{-3}$ for Polystyrene. ϵ^{-} is the efficiency of the apparatus to detect the gamma rays. There is no need here to include a quantity corresponding to ϵ_g as in (3) because the reaction (4) is a strong interaction and is, therefore, prompt.

ϵ^{-} is not equal to its counterpart ϵ^{+} since the neutral pions from (4) have a different velocity distribution from those arising from (1). Therefore, the angular distributions of the decay gamma rays as well as their energy spectra will differ and consequently so will the detection efficiencies. However, the reaction (5) can be used to obtain a value for ϵ^{-} and the ratio $\rho\equiv\epsilon^{+}/\epsilon^{-}$ used in conjunction with (3) to arrive at a value of R. As will be shown, ρ can be computed by the Monte Carlo technique if certain reasonable assumptions are made.

B. Data Collected

Three types of data were needed to provide the information necessary to arrive at a measurement of the branching ratio R:

(a) Positive particles stopping and the apparatus triggered by the signature $\pi\gamma\gamma$ as described in Sec. IIA. These data contain events which are examples of reaction (1).

(b) Negative particles stopping and the electronics set to give a $\pi\gamma\gamma$ trigger but with the π gate not delayed (and the $\bar{1}\bar{\gamma}\bar{\gamma}$ anticoincidence removed). This made the apparatus sensitive to reaction (4).

(c) Positive or negative particles stopping, using the coincidence $123\bar{4}$ as a trigger. These data were needed to give information on the spatial distribution of stopping particles, which was then used to define the fiducial regions and also to provide corrections to the scaler readings when determining the number of useful pion.

Oscilloscope pictures were taken for types (a) and (b) but not for type (c).

The various types of data were taken in a mixed order so that a continuous check on the condition of the spark chambers and the electronics was obtained. The system proved to be very stable so that essentially no adjustments were necessary. 1.46×10^{11} particles were stopped and 40 000 pictures were taken during the π^{+} run. An equal number of pictures were taken of π^{-} charge exchanges.

C. Scanning and Measuring

For events of type (a) the spark-chamber photographs were examined by scanners with the help of a set of scanning rules. Frames which passed the rules were measured either by hand or with the aid of a digitizing machine. The measurement consisted of obtaining

[14] A. F. Dunaitzev, Yu. D. Prokoshkin, and Tang Syao-Wei, Nucl. Instr. Methods 8, 11 (1960).

[15] M. Chabre, P. DePommier, J. Heintze, and V. Soergel, Phys. Letters 5, 67 (1963).

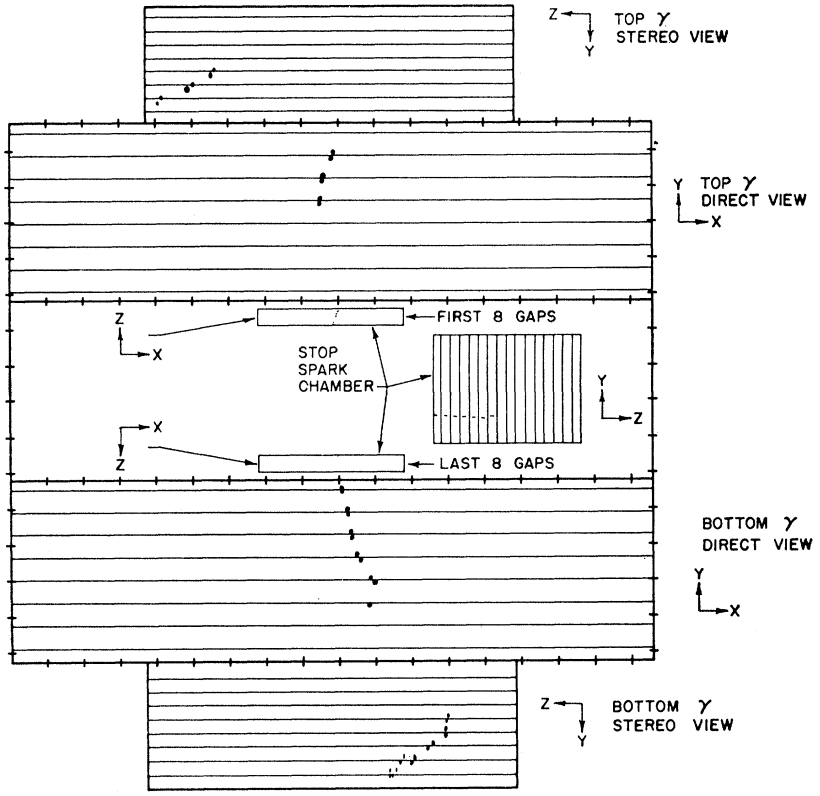

FIG. 3. Facsimile of a typical candidate for pion beta decay.

the coordinates of three points: P_s the point at which which the pion stopped, $P_{\gamma t}$ and $P_{\gamma b}$ the points at which the gamma rays converted. These points were used to reconstruct the event in space and to compute the opening angle $\theta_{\gamma\gamma}$. This was done with a computer program on an IBM-7040 digital computer, at Carnegie Institute of Technology. Those events which resulted in $|\cos\theta_{\gamma\gamma}| \geqslant 0.96 (\theta_{\gamma\gamma} > 163.7^0)$ were then re-examined at the scanning table by a physicist. The choice of a cutoff eliminated events which surely were not possible candidates for $\pi^+\beta$ decay and yet provided a sufficiently large region outside the range where these events could be expected to fall, to permit a good determination of the background. At this time the oscilloscope film was also examined, and a check was made for the presence of an antipulse or multiple stops. The time between the occurrence of a stop and the detection of the electrons from gamma-ray conversion $t_{\pi\gamma}$ was measured for those frames which were acceptable. The events were subjected to a further selection by considering the angle between the direction of the gamma ray and the average direction of the conversion electrons $\theta_{\gamma e}$. This will be described in detail below. Events which survived all these tests constituted the final sample of $\pi^+\beta$ decays plus background. Events of type (b) were treated in the same manner as those of type (a) except that no cutoff on $\theta_{\gamma\gamma}$ was applied.

The stopping chamber was examined first. If the track was acceptable, then the two gamma chambers were scanned. The following rules applied to the stopping chamber.

(i) Only one track must be present.

(ii) A track must be at least three sparks and no more than 14 sparks long. It must also be more than $\frac{1}{4}$ in. from the sides of the chamber.

(iii) No more than two missing sparks must occur, and these must not be consecutive.

Requirements for tracks in the gamma chambers were:

(i) Tracks must pass through at least four gaps, and three out of the first four gaps must have sparks in them.

(ii) The sparks must form a coherent group in both views.

(iii)For events of type (a), the projection of $\theta_{\gamma\gamma}$ onto the x-y plane must be greater than 155 deg. The projected angle is defined as the lesser angle between the two lines $P_sP_{\gamma t}$ and $P_sP_{\gamma b}$. Although, in principle, this angle can range between 0 and 180 deg, the actual range is restricted by the geometry of the apparatus and in fact the above choice of limit meant that events outside the criterian could not have $\theta_{\gamma\gamma} > 163$ deg. The projected angle could easily be measured directly on the scanning table with a protractor. The limit served to eliminate the measurement of events which surely could not be candidates for real positive pion decays. A facsimile of a good event is shown in Fig. 3. Out of a total of 40 650 frames of type (a) taken 3286 were measured and computed, and 330 had $|\cos\theta_{\gamma\gamma}| \geqslant 0.96$.

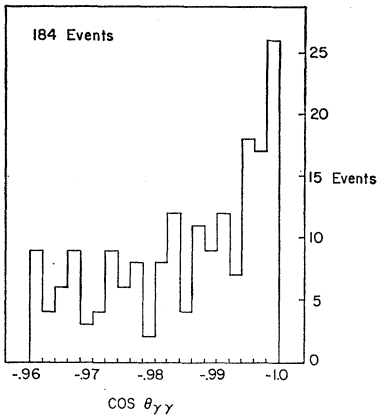

FIG. 4. Distribution of all events (184) satisfying the scanning rules and oscilloscope trace criteria.

After these were examined by a physicist, 184 survived and are shown in Fig. 4.

D. Efficiencies

The efficiency ϵ^+ [Eq. (3)] can be factored into a number of parts: $\epsilon^+ = \epsilon_{gc}{}^+\epsilon_p{}^+\epsilon_b{}^+\epsilon_e{}^+\epsilon_s{}^+$, where ϵ_{gc} is the geometrical and conversion efficiency (this was calculated by a Monte Carlo program to be about 15%), $1-\epsilon_p{}^+$ represents the fraction of events in which at least one gamma ray converted in material before reaching the gamma detector and was vetoed by the anticounters, $1-\epsilon_b{}^+$ refers to those cases in which after conversion one of the electrons scattered backwards and entered one of the anticounters, $\epsilon_e{}^+$ represents the electronic efficiency, and $\epsilon_s{}^+$ stands for a seeing efficiency which measures the ability to recognize the group of sparks, formed by the conversion electrons, as a good "gamma." ϵ^-[Eq. (5)] can be factored in a similar manner. We have assumed that the only significant difference between ϵ^+ and ϵ^- lies in the geometry-conversion efficiency factors and that therefore $\rho \equiv \epsilon^+/\epsilon^- = \epsilon_{gc}{}^+/\epsilon_{gc}{}^-$, i.e., all the other factors going into the efficiencies cancel out to first order when forming the ratio. The ratio $\epsilon_{gc}{}^+/\epsilon_{gc}{}^-$ was easily computed with a Monte Carlo program, and the result was $\rho = 1.20$. The error in ρ arising out of the calculation itself was made very small by choosing many trials.

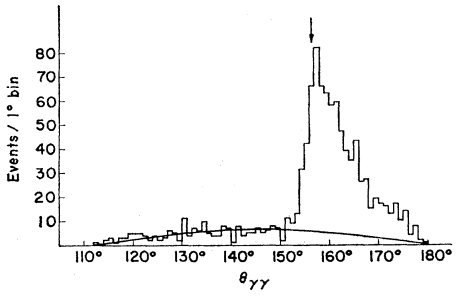

FIG. 5. Opening-angle distribution of 1037 charge-exchange events. The smooth curve indicates the charge exchange in flight background.

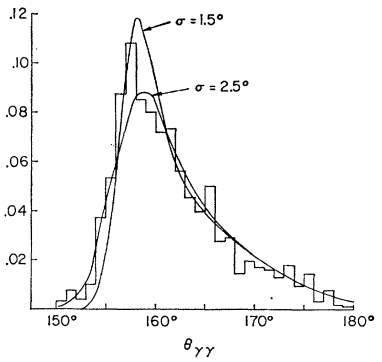

FIG. 6. Opening-angle resolution curves from charge-exchange data after charge exchange in flight has been subtracted. The histogram contains 743 events. The smooth curves result from computation of the theoretical distribution with Gaussian measurement errors folded in.

As mentioned earlier, ϵ^- was obtained from the data of type (b). Figure 5 shows a sample of events of this type. The smooth curve represents events which we believe are charge exchanges in flight and should therefore be subtracted. The results after subtraction are shown in Fig. 6 and compared with several theoretical curves, which have errors in the determination of the opening angle folded into them. This was done by multiplying the theoretical opening-angle distribution[16] by a Gaussian function characterized by a standard deviation σ, and then integrating over the opening angle. As seen in Fig. 6, $\sigma = 2$ deg would fit the data rather nicely. A direct examination of the raw data of Fig. 5 or Fig. 6 also shows that this estimate is reasonable since the data falls to background in about three bins to the left of the peak (each bin is one degree). The approach towards the errors just discussed does not apply in the region about 180 deg for several reasons. In the first place the error in $\theta_{\gamma\gamma}$ is actually compounded from errors in the measurement of P_s, $P_{\gamma t}$, and $P_{\gamma b}$ and is not a simple one-dimensional function of $\theta_{\gamma\gamma}$ as was described above. Secondly, in the neigh-

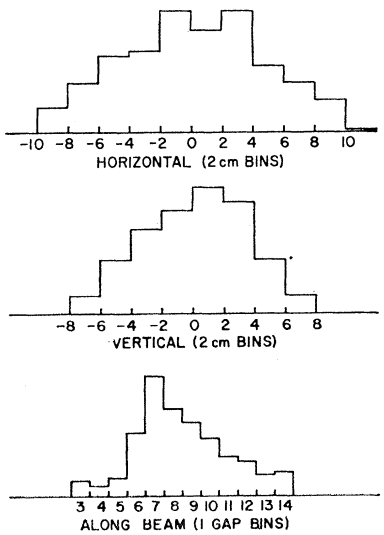

FIG. 7. Samples of the distributions for stopping particles.

[16] See, for example, B. B. Rossi, *High-Energy Particles* (Prentice-Hall Inc., New York, 1952), p. 197.

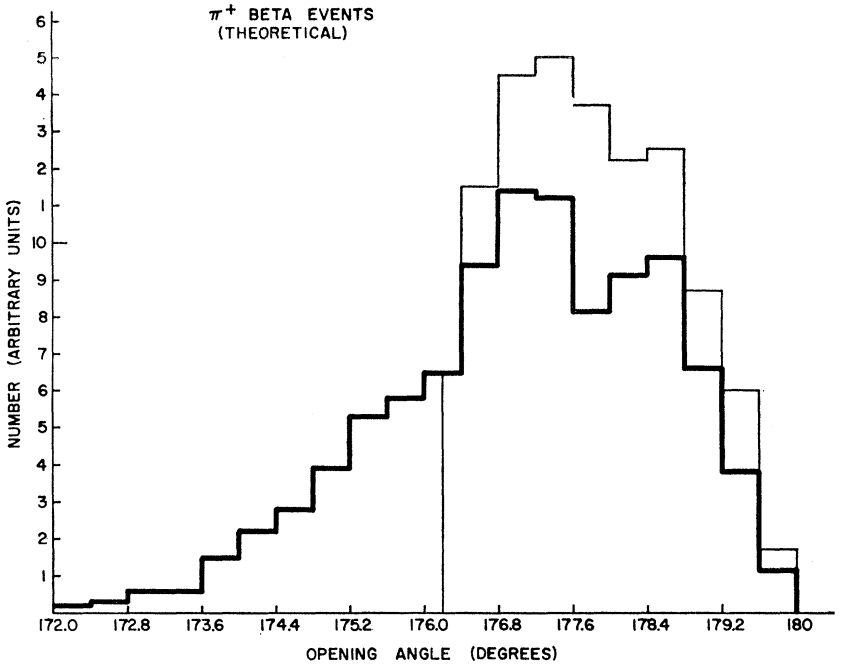

FIG. 8. Monte Carlo calculations of the expected distribution of $\pi\beta$ events. The light histogram has the momentum distribution of the neutral pion folded in. The bold histogram includes measurement errors in addition to the neutral pion momentum distribution.

borhood of 180-deg errors can only be in such a direction as to make the opening angle smaller, since 180 deg is the largest possible angle. To treat the problem more correctly, a more sophisticated Monte Carlo program was devised. For this calculation it was assumed that the z coordinate of P_s was uniformly distributed over $\frac{1}{4}$ in. and that the x and y coordinates were distributed in Gaussian manner with $\sigma=1$ mm. The conversion points P_γ were assumed to be distributed in Gaussian manner with $\sigma_x=2$ mm, $\sigma_y=0.1$ mm, and $\sigma_z=3$ mm. This combination was one of several tried and was in agreement with the charge-exchange data. As will be shown below, the final selection of $\pi^+\beta$ events agreed well with a histogram generated using these errors.

ϵ_g was calculated by folding the experimental-decay curve for pions into the shape of the gate curve. The shape of this curve was obtained by counting $\pi^-\gamma\gamma$ events (charge exchange) as a function of gate delay. If $g(t)$ represents the gate shape and τ_π the pion mean life, then ϵ_g is given by

$$\epsilon_g=\frac{1}{\tau_\pi}\int_0^\infty g(t)\exp(-t/\tau_\pi)dt. \tag{6}$$

The number of stopping pions $N_\pi{}^\pm$ [Eqs. (3) and (5)] was obtained from the type (c) data in conjunction with measurements of the beam contamination discussed earlier (Sec. IIB). The photographs were scanned according to the rules established for the stopping chamber. No computation was needed here as the coordinates could be measured directly on the scanning table. A sample of distributions resulting from this scan are shown in Fig. 7. These were used to determine the number of stops in the chosen fiducial volume. $N_\pi{}^\pm$ were determined by multiplying the $123\bar{4}$ scalar readings by the fraction of good stops in a given fiducial volume and by the fraction that are pions.

A correction for scanning efficiency must also be made. The important factor that enters into the branching ratio calculation is the ratio of the scanning efficiency

TABLE I. Factors affecting the detection efficiency and related quantities.

Corrections to beam intensity:	
No. of $123\bar{4}$ coincidences	146.2×10^9
Fraction in fiducial volume	0.66 ± 0.035
Fraction of fiducial volume stops that are pions	0.98 ± 0.01
$N_\pi{}^+$	$(94.6\pm4.7)\times10^9$
Efficiency factors:	
$\rho=\epsilon^+/\epsilon^-$	1.20
ϵ^+	0.0608 ± 0.008
ϵ_g	0.56 ± 0.03
Scanning eff. (ratio π^-/π^+)	1.03 ± 0.02
Total efficiency	0.0330 ± 0.0046

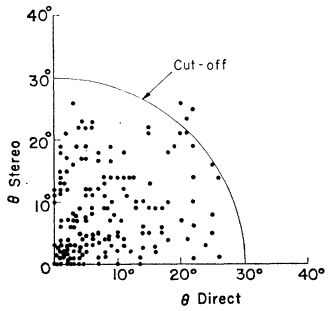

FIG. 9. Distribution of projected angles between the gamma-ray direction and the direction of the conversion products for charge-exchange events.

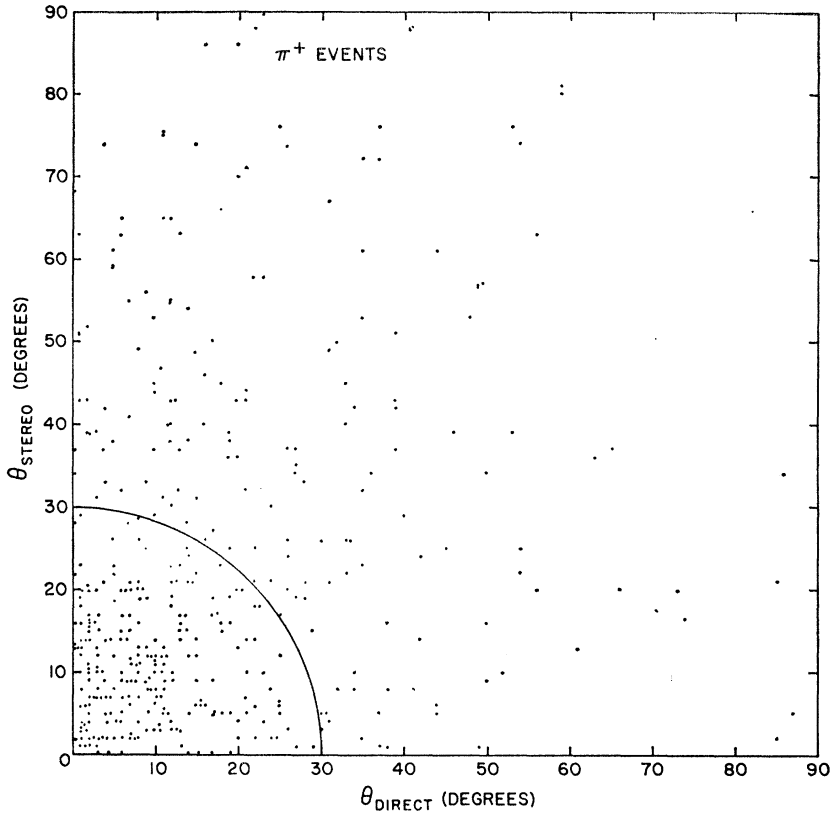

FIG. 10. Distribution of projected angles between the gamma-ray direction and the direction of the conversion electrons for pion beta-decay candidates.

for π^- charge-exchange events to that for $\pi^+\beta$ decay events. That this ratio is not equal to one is reasonable because in the π^- pictures 60% of the frames are measured events while in the π^+ pictures only about 10% are measured. By doing an independent second scan on a sample of the data, it was found that eff(π^- pictures)/eff(π^+ pictures) $=1.03\pm0.02$. A summary of the factors entering into the detection efficiency is presented in Table I.

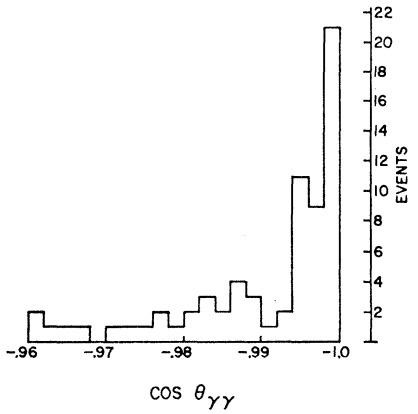

FIG. 11. Opening-angle distribution of final candidates (69) for pion beta-decay events.

E. Correlation Between Gamma Rays and Electron-Positron Pairs

After the application of the various criteria described in Sec. IIIC, we are left with 184 events as candidates for reaction (1), shown in Fig. 4. This sample contains background as well as real $\pi^+\beta$ decays. Figure 8 shows the results of a Monte Carlo calculation of the expected distribution of opening angles for $\pi\beta$ events. This was computed by folding the known momentum spectrum of neutral pions from reaction (1) into the opening-angle distribution for $\pi^0\rightarrow\gamma+\gamma$ decay.[16] Also shown in Fig. 8 is the result of modifying the aforementioned expected distribution by the inclusion of errors (Sec. III C) in determining $\theta_{\gamma\gamma}$. As can be seen, essentially no events are expected below $|\cos\theta_{\gamma\gamma}|=0.99$ even when errors are considered. On the other hand, Fig. 4 shows quite a few cases below this limit, indicating that considerable background is included in the sample of 184 events. An attempt to reduce the background further was made by using the angle $\theta_{\gamma e}$ between the gamma-ray line P_sP_γ and the average direction of the conversion electrons. The average direction of the conversion pair was defined by the best straight line through the first four sparks in the track. The two projections of $\theta_{\gamma e}$: the direct or x-y projection $(\theta_{\gamma e})_d$, and the stereo or y-z projection $(\theta_{\gamma e})_s$, were plotted for gamma rays from events of types (a) and (b). The results for a sample of

charge-exchange gammas are shown in Fig. 9 (one event contributes two points to the plot). As can be seen from Fig. 6, there is essentially no background in the charge-exchange events and so these can be used to establish a connectedness criterion for gamma rays and their associated electron-positron pairs. A circle of radius 30 deg retains almost all of the events. Figure 10 shows a sample of gamma rays from $\pi^+\beta$ decay candidates. As can be seen, there are many points outside the 30-deg limit. When this criterion is applied to the 184 events, a drastic reduction in background events occurs without materially affecting the events in region above $|\cos\theta_{\gamma\gamma}|=0.99$. This fact enhances our confidence in this method of background reduction. The results are shown in Fig. 11.

IV. RESULTS AND CONCLUSIONS

Figure 11 contains the final sample of 69 candidates for reaction (1). According to Fig. 8 true events are expected only in the region $0.99\leqslant|\cos\theta_{\gamma\gamma}|\leqslant|$. It was assumed that the residual background was isotropic (i.e., flat in $\cos\theta_{\gamma\gamma}$). The region $0.96\leqslant|\cos\theta_{\gamma\gamma}|<0.99$ was used to determine this background which was then subtracted from the events in the region above $\cos|\theta_{\gamma\gamma}|=0.99$.

TABLE II. Calculation of the branching ratio.

Events with $\|\cos\theta_{\gamma\gamma}\|>0.99$	44
Events with $0.96\leqq\|\cos\theta_{\gamma\gamma}\|<0.99$	25
Net No. of $\pi^+\beta$ events	35
Branching ratio R	$(1.10\pm0.26)\times10^{-8}$

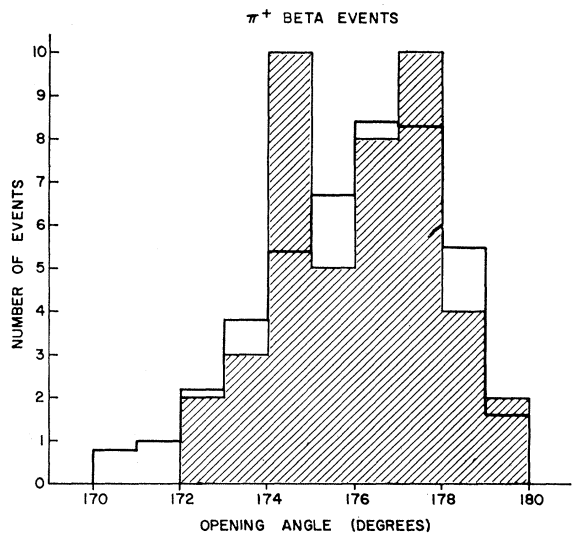

FIG. 12. 44 events with $|\cos\theta_{\gamma\gamma}|>0.99$ (shaded area). The bold histogram is the theoretically expected distribution and is identical to the corresponding histogram in Fig. 8, but normalized to 44 events.

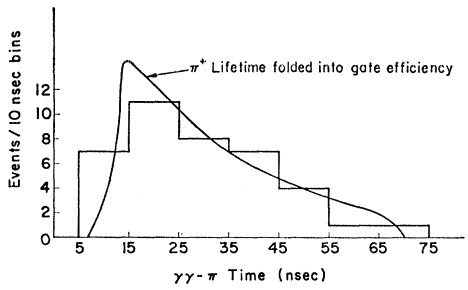

FIG. 13. Observed time distribution of 39 pion beta-decay events. The smooth curve is computed according to Eq. (6).

Following this the information of Table I and Eq. (3) were used to compute R. This procedure is summarized in Table II and the final group of accepted pion beta-decay events shown in Fig. 12. The error in R can be broken into several terms: 20% from the number of observed $\pi^+\beta$ decay events, 15% from the efficiency (most of this error is contained in the branching ratio for charge-exchange R_{ce}), and 5% from the effective number of stopping pions (N_π).

The final result is in agreement with both the CVC and Cabibbo prediction, as well as with other experimental results which are summarized in Table III.

TABLE III. Summary of $\pi^+\beta$ experiments.

Group	Detector	Events	$R\times10^8$
CERN[a]	Lead glass Čerenkov	52±3	1.15±0.22
Dubna[a]	Total absorption Čerenkov	43±5	1.1 ±0.2
Columbia[b]	Spark chambers	36±1	0.97±0.20
CERN[c]	Lead glass Čerenkov	165±5	1.17±0.12
This exp.	Spark chambers	35±3	1.10±0.26

[a] See Ref. 10.
[b] See Ref. 12.
[c] See Ref. 11.

The time distribution of all events in the region, $|\cos\theta|>0.99$, is shown in Fig. 13 along with the expected distribution obtained by folding the pion lifetime into the gate efficiency. There were actually 44 events in this region, but 5 of them did not have scope pictures because of various mechanical malfunctions. These events were included in the good-event category, but in calculating the branching ratio they were weighted with the probability that the scope film would throw them out.

ACKNOWLEDGMENTS

We would like to thank graduate students: P. D. Gupta, D. Sashin, N. Dickman, and A. Gaigalas; technicians: R. Harbison and R. Mead; and scanners: J. Gianneschi and C. Rothen for their important contributions to this experiment. In addition, the help of the operating staff of the Nuclear Research Center is gratefully acknowledged.